

A harmonic analysis of 100 mb zonal winds in the tropics

J. M. WALKER

Department of Maritime Studies,

University of Wales Institute of Science and Technology, Cardiff. (U.K.)

(Received 12 August 1974)

ABSTRACT. Monthly-mean 100 mb zonal wind observations from stations in, or on the fringe of, the tropics have been subjected to Fourier analysis.

Annual and semi-annual harmonics are evident at many stations, and superpositions of these two harmonics reproduce observations quite well at these stations. Dates corresponding to greatest rates of change of zonal-wind velocity coincide well with the onset and retreat of summer monsoon circulations, except over the western North Pacific Ocean, where the annual harmonic behaves rather differently from elsewhere. It is clear that upper easterlies associated with summer monsoon circulations influence upper-wind patterns well beyond those areas generally considered to be monsoonal on the basis of rainfall and surface-wind reversals.

1. Introduction

It is well-known that reversals of direction of the upper-tropospheric flow over the tropics of the eastern hemisphere are associated with the onset and retreat of summer monsoon circulations; the westerlies which prevail for much of the year are replaced by easterlies for about four months each summer.

The abruptness of the reversals prevents such flow-patterns from being described correctly as harmonic oscillations. Instead, it is more accurate to consider what Hantel (1971), discussing the annual march of temperature over southern Asia, termed 'a flipflop-like oscillation between relatively steady states, with discontinuous jumps from one state to another'. Even so, it is not precise to use the description 'discontinuous' for upper-wind patterns. Reversals are rapid, as Fig. 1 shows, but they are not sufficiently precipitous or smooth for dates corresponding to transitions to be determined exactly by visual inspection of daily data. Accordingly, some statistical procedure must be adopted to establish average dates.

Flow patterns of this kind are, as Hantel pointed out, 'characterised by sizeable contributions of higher harmonics'. However, as he was advised (by H. Van Loon) that harmonics higher than the semi-annual do not contribute significantly to the total variance of temperature, Hantel felt justified in describing the zonally-averaged

annual patterns of temperature between 60° and 120°E in terms of superpositions of annual and semi-annual harmonics.

2. Outline of Investigation

The present study, a harmonic analysis of monthly-mean 100-mb zonal-winds at 45 stations in, or on the fringe of, the tropics (see Fig. 2 and Appendix), showed that there is in addition to the anticipated, and usually considerable, annual harmonic, a conspicuous semi-annual harmonic present in the data of many stations (Table 1). Indeed, at some stations in the Southern Hemisphere the amplitude of the semi-annual harmonic exceeds that of the annual, a fact which has been discussed at length by Van Loon and Jenne (1969, 1970). Harmonics higher than the semi-annual do not contribute greatly to the total variance of zonal-wind at most stations and superpositions of annual and semi-annual harmonics reproduce 100-mb zonal-wind observations tolerably well in general (Fig. 3). However, at some stations harmonics lower than the annual are evident, while at Cocos Island the amplitude of the biennial harmonic exceeds that of the annual.

It was hoped initially that this study would provide insight into inter-annual variations of monsoon intensity. In particular, it was thought possible that some influence from the quasi-biennial oscillation might be apparent, and

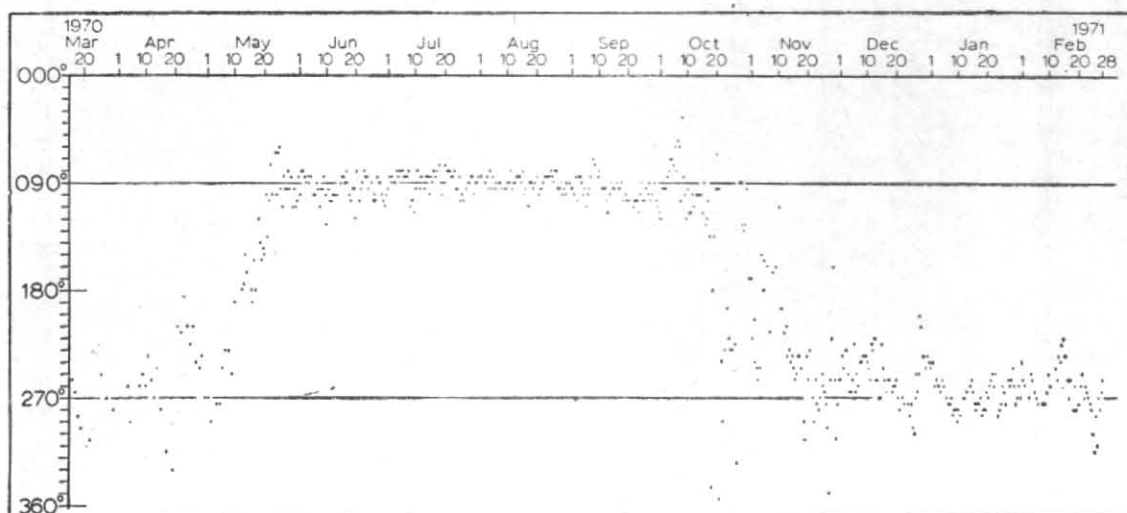


Fig. 1. Wind directions at 100 mb over Masirah Island ($20^{\circ}30'N$, $58^{\circ}40'E$), at 00 and 12 GMT between 15 March 1970 and 28 February 1971, illustrating the nature of the transitions between winter and summer flows

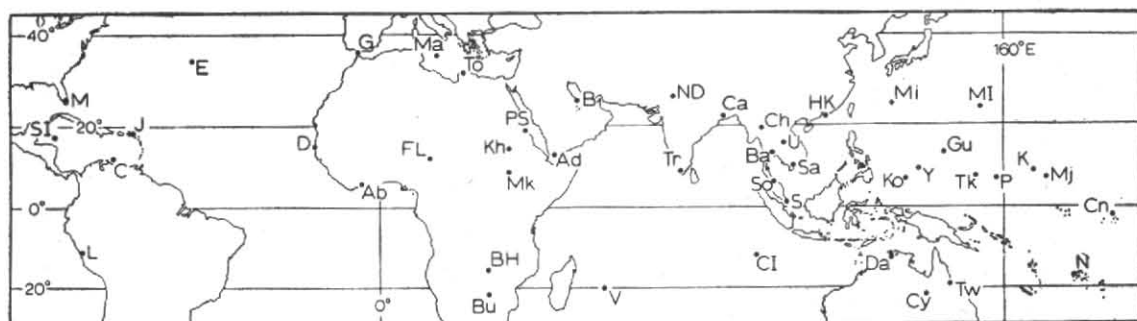


Fig. 2. Location of stations used in this study

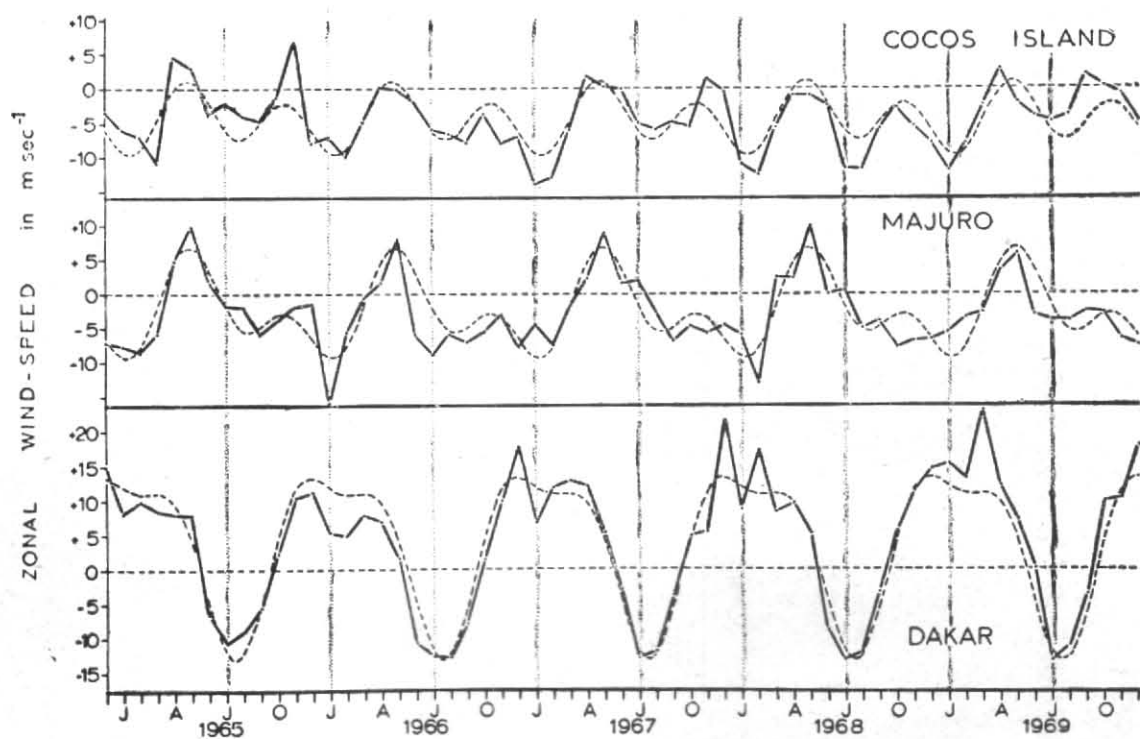


Fig. 3. Comparison between 100-mb zonal-wind observations (continuous lines) and superpositions of annual and semi-annual harmonics (dotted lines) at Cocos Island, Majuro and Dakar

TABLE 1
Proportion of total variance due to major harmonics,
in per cent

Station	Annual and semi-annual combined	Annual alone	Semi-annual alone
<i>Northern Hemisphere</i>			
Aden	97.7	88.1	9.6
Bahrein	97.2	93.0	4.2
Bangkok	94.9	91.1	3.8
Calcutta	96.9	94.3	2.6
Chiengmai	96.3	93.7	2.6
Curacao	72.6	42.2	30.4
Dakar	94.5	83.2	11.3
Fort Lamy	76.0	69.0	7.0
Guam	78.5	71.1	7.3
Hong Kong	96.9	95.7	1.2
Juliana	91.2	70.7	20.5
Khartoum	95.0	87.0	8.0
Koror	75.5	55.5	19.9
Kwajalein	86.0	56.6	29.3
Majuro	82.5	49.7	32.8
Miami	96.7	94.9	1.8
New Delhi	96.9	94.2	2.8
Ponape	82.2	56.2	26.0
Port Sudan	95.4	89.4	6.1
Saigon	92.1	87.6	4.5
Songkhla	87.8	80.5	7.3
Swan Island	88.3	85.6	2.8
Trivandrum	93.4	90.3	3.1
Truk	83.7	61.7	22.0
Ubon Ratchathani	95.0	92.0	3.0
Yap	76.1	59.9	16.3
<i>Southern Hemisphere</i>			
Broken Hill	79.1	46.8	32.3
Bulawayo	77.5	61.9	15.6
Canton Island*	54.3	34.1	20.2
Cloncurry	73.7	47.1	26.6
Cocos Island*	62.2	12.4	49.8
Darwin	87.8	39.7	48.1
Lima	85.1	77.5	7.6
Nandi	80.6	57.5	23.1
Townsville*	61.0	36.5	24.6
Vacoas	93.1	15.4	77.8

*At these stations there are other harmonics contributing more than 10 per cent of the total variance, thus :

Canton Island	Cycle of 28 months	17.7 per cent
Cocos Island	24 months	16.2 per cent
Townsville	72 months	14.4 per cent

it was for this reason that 100-mb was chosen, being a level both typical of upper tropospheric wind patterns and perhaps likely to yield some evidence of the oscillation. This hypothesis was discarded when evidence for a significant near biennial harmonic appeared in the data of only two stations, Cocos Island and Canton Island, both some distance from recognised monsoonal centres of action.

Nevertheless some interesting consistencies and inconsistencies in the temporal and spatial characteristics of reversals and of annual and semi-annual harmonics emerged from the study, and it is these which provide the *raison d'être* of this paper.

3. Data

The 100-mb wind observations were extracted from the United States Department of Commerce publication *Monthly Climatic Data for the World* and for each station expressed as a Fourier series in the form :

$$u = \frac{1}{2} a_0 + \sum_n^N c_n \sin \left(\frac{2\pi n t}{T} + \delta_n \right) \quad (1)$$

where,

u = zonal velocity, westerlies positive,

t = time in months,

T = length of record analysed, in months,

c_n^2 = sum of the squares of the usual Fourier coefficients a_n and b_n

δ_n = the phase relationship, $\tan^{-1} (a_n/b_n)$

The number of observations available for analysis varies from station to station (see Appendix), so a test was performed upon the observations from Bahrein to determine the minimum length of record which yields reliably the amplitudes and phases of the major components, the annual and semi-annual harmonics. These amplitudes and phases were computed for $T = 12$ (12) 132 (T was analysed in steps of 12 months from 12 to 132, *i.e.*, the amplitudes and phases were computed for $T = 12, T = 24, T = 36$ etc) and it was decided thereby that stations for which only 36 consecutive observations were available would be acceptable (see Fig. 4).

4. Analysis

At all but Cocos Island of the stations listed in Table 1 the annual and semi-annual harmonics each make greater contributions to the total variance than any other harmonics. For these stations, and including Cocos Island, despite its large biennial harmonic, Eq. (1) was reduced to :

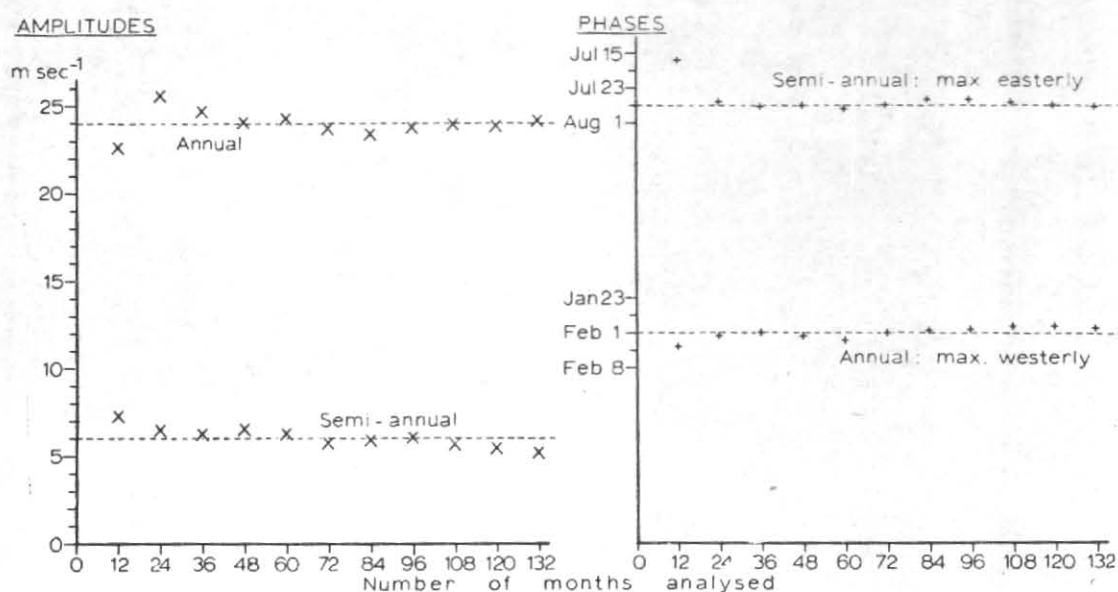


Fig. 4. Amplitudes and phases of annual and semi-annual harmonics at Bahrain for $T=12(12) 132$

$$u = \frac{1}{2} a_0 + A \sin \frac{2\pi}{12}(t + \phi) + B \sin \frac{4\pi}{12}(t + \psi) \quad (2)$$

where, A and B , ϕ and ψ , are the amplitudes and phases of the annual and semi-annual harmonics respectively. Hence, the second derivative was obtained:

$$\frac{d^2u}{dt^2} = -\left(\frac{2\pi}{12}\right)^2 \left[A \sin \frac{2\pi}{12}(t + \phi) + 4B \sin \frac{4\pi}{12}(t + \psi) \right] \quad (3)$$

Then, for each station, the values of t for which $d^2u/dt^2 = 0$ were computed, so identifying dates corresponding to greatest rates of change of zonal-wind speed in Eq. (2). Observations yielded four such values of t at all Southern Hemisphere stations and at many of the Northern Hemisphere stations, but only two such values of t at the remainder of the Northern Hemisphere stations (where the second harmonic was small).

At Abidjan and Singapore several harmonics are conspicuous, and it is clear that this would have been the case also at the East African equatorial stations Entebbe and Nairobi had there been sufficient consecutive observations to allow quantitative analysis. At each of the other stations not listed in Table 1, there is a considerable annual harmonic but no significant semi-annual harmonic.

5. The first and second derivatives

Dates corresponding to $d^2u/dt^2 = 0$, associated

values of du/dt and dates during northern summer when $du/dt = 0$ are listed in Table 2. The principal features are, briefly:

(i) All stations display a solution of $d^2u/dt^2 = 0$ within the period 15 September to 15 October. Only at Lima is the value of du/dt not positive for this solution, and at several Asian and North African stations du/dt exceeds 10 m/sec/month. Large values of du/dt over southern Asia and North Africa at this time are not unexpected, for they correspond to the cessation of summer monsoon activity and the associated reversal of upper winds from easterly to westerly.

Strüning and Flohn (1969) have drawn attention to the extraordinary width of upper tropospheric easterlies during northern summer and have mentioned that they some times extend from 27°N to 12°S above the Indian Ocean and East Africa. These upper easterlies over the South Indian Ocean and adjacent lands weaken or reverse to light westerly when the monsoon of southern Asia retreats, the suggestion from the solutions of $d^2u/dt^2 = 0$ being that the transition occurs a few days earlier in the Southern Hemisphere than in the Northern.

(ii) The reversal of upper winds from westerly to easterly which accompanies the onset of summer monsoon activity over southern Asia and North Africa is revealed by solutions of $d^2u/dt^2 = 0$ in late May or early June over these areas, and associated values of du/dt are again mostly large, exceeding -10 m/sec/month at several stations.

TABLE 2

Dates corresponding to $d^2u/dt^2=0$ associated values of du/dt and dates during northern summer when $du/dt=0$

Station	$d^2u/dt^2=0$ and, in brackets, du/dt in m/sec/month				$du/dt=0$
<i>North Africa and Arabia</i>					
Aden	Sep 24 (13.7)	May 30 (-13.6)	Jan 3 (-0.8)	Feb 21 (0.7)	Jul 27
Bahrein	Sep 33 (15.3)	May 27 (-15.9)	—	—	Jul 27
Dakar	Sep 30 (10.1)	Jun 6 (-9.2)	Jan 9 (-1.7)	Mar 3 (0.2)	Aug 3
Fort Lamy	Sep 27 (7.4)	May 30 (-8.0)	Jan 3 (+0.1)	Feb 18 (0.9)	Jul 30
Khartoum	Sep 24 (12.6)	May 27 (-13.6)	Jan 3 (+0.4)	Feb 12 (1.3)	Jul 27
Port Sudan	Sep 30 (15.9)	May 30 (-15.6)	Jan 21 (-0.3)	Feb 9 (-0.2)	Jul 30
<i>Asia</i>					
Bangkok	Sep 21 (8.2)	May 18 (-11.3)	—	—	Jul 24
Calcutta	Oct 3 (14.3)	May 24 (-13.7)	—	—	Jul 27
Chiengmai	Sep 30 (11.9)	May 21 (-14.2)	—	—	Jul 27
Hong Kong	Oct 9 (12.3)	May 18 (-12.5)	—	—	Jul 30
New Delhi	Oct 6 (12.3)	May 27 (-9.7)	—	—	Jul 30
Saigon	Sep 21 (4.9)	May 18 (-7.9)	Dec 6 (+2.8)	Jan 12 (3.0)	Jul 21
Songkhla	Sep 15 (5.7)	May 21 (-6.8)	Dec 21 (+0.7)	Feb 3 (1.2)	Jul 18
Trivandrum	Sep 27 (6.5)	May 21 (-7.0)	—	—	Jul 21
Ubon	Sep 27 (9.1)	May 18 (-11.4)	—	—	Jul 27
Ratchathani					
<i>Central America</i>					
Curacao	Sep 30 (5.0)	Jun 18 (-5.4)	Dec 27 (-2.0)	Mar 15 (2.5)	Aug 9
Juliana	Oct 3 (6.5)	Jun 15 (-7.3)	Jan 3 (-1.2)	Mar 9 (2.3)	Aug 9
Miami	Oct 9 (9.1)	May 24 (-10.1)	—	—	Aug 3
Swan Island	Oct 15 (5.8)	Jun 6 (-5.7)	—	—	Aug 9
<i>Western North Pacific</i>					
Guam	Oct 9 (1.6)	Jun 18 (-4.4)	Dec 6 (+0.8)	Feb 24 (2.8)	Aug 27
Koror	Sep 24 (0.9)	Jun 24 (-3.9)	Dec 3 (-1.4)	Mar 9 (4.2)	Aug 27
Kwajalein	Sep 30 (1.6)	Jul 3 (-5.4)	Dec 15 (-2.8)	Mar 21 (6.3)	Aug 30
Majuro	Sep 24 (2.0)	Jun 30 (-5.8)	Dec 12 (-3.6)	Mar 18 (7.1)	Aug 27
Ponape	Sep 24 (1.1)	Jun 30 (-4.9)	Dec 9 (-4.0)	Mar 21 (7.2)	Aug 30
Truck	Sep 27 (0.7)	Jul 6 (-4.4)	Dec 12 (-3.3)	Mar 21 (6.5)	Sep 6
Yap	Oct 6 (1.6)	Jun 27 (-4.5)	Dec 12 (-0.4)	Mar 9 (3.7)	Aug 30
<i>Southern Hemisphere</i>					
Broken Hill	Sep 15 (1.8)	Jun 27 (-3.7)	Dec 12 (-5.1)	Mar 21 (6.7)	
Bulawayo	Sep 27 (0.02)	Jul 9 (-4.2)	Dec 9 (-3.8)	Mar 24 (7.1)	
Canton Island	Sep 27 (3.2)	Jun 18 (-5.2)	Dec 18 (-1.1)	Mar 9 (3.5)	
Cloncurry	Sep 27 (2.1)	Jul 9 (-4.6)	Dec 21 (-7.1)	Apr 3 (9.1)	
Cocos Island	Sep 21 (3.1)	Jun 21 (-4.3)	Dec 15 (-4.0)	Mar 18 (5.1)	
Darwin	Sep 18 (3.8)	Jun 27 (-5.6)	Dec 15 (-7.7)	Mar 21 (9.3)	
Lima	Oct 6 (-1.7)	Jul 30 (-3.9)	Dec 12 (-3.8)	Apr 6 (7.6)	
Nandi	Sep 27 (1.8)	Jul 15 (-1.6)	Dec 30 (-5.6)	Apr 12 (5.5)	
Townsville	Sep 27 (2.0)	Jul 9 (-3.9)	Dec 21 (-5.7)	Apr 3 (7.3)	
Vacoas	Sep 18 (5.8)	Jun 24 (-6.1)	Dec 18 (-8.0)	Mar 24 (8.3)	

TABLE 3

Dates corresponding to $\sin \frac{2\pi}{12}(t+\phi)=+1$ and $\sin \frac{4\pi}{12}(t+\phi)=-1$

Station	$\sin \frac{2\pi}{12}(t+\phi)$ = +1	$\sin \frac{4\pi}{12}(t+\phi)$ = -1
<i>North Africa and Arabia</i>		
Aden	Jan 27	Jan and Jul 27
Bahrein	Jan 30	Jan and Jul 27
Dakar	Jan 27	Feb and Aug 6
Fort Lamy	Feb 3	Jan and Jul 27
Khartoum	Jan 30	Jan and Jul 24
Port Sudan	Jan 30	Jan and Jul 30
<i>Asia</i>		
Bangkok	Feb 3	Jan and Jul 9
Calcutta	Jan 27	Jan and Jul 30
Chiengmai	Feb 3	Jan and Jul 21
Hong Kong	Jan 30	Jan and Jul 27
New Delhi	Jan 21	Feb and Aug 9
Saigon	Feb 9	Jan and Jul 6
Songkhla	Jan 27	Jan and Jul 15
Trivandrum	Jan 27	Jan and Jul 21
Ubon Ratchathani	Feb 3	Jan and Jul 15
<i>Central America</i>		
Curacao	Feb 18	Feb and Aug 9
Juliana	Feb 18	Feb and Aug 9
Miami	Feb 6	Jan and Jul 27
Swan Island	Feb 9	Feb and Aug 9
<i>Western North Pacific</i>		
Guam	Mar 30	Jan and Jul 30
Koror	May 9	Jan and Jul 30
Kwajalein	May 24	Feb and Aug 9
Majuro	May 30	Feb and Aug 6
Ponape	Jun 12	Feb and Aug 6
Truk	Jun 12	Feb and Aug 9
Yap	Apr 18	Feb and Aug 6
<i>Southern Hemisphere</i>		
Broken Hill	Jul 6	Feb and Aug 3
Bulawayo	Jun 21	Feb and Aug 9
Canton Island	Mar 21	Feb and Aug 3
Cloncurry	Jul 21	Feb and Aug 15
Cocos Island	Jun 9	Feb and Aug 3
Darwin	Jul 12	Feb and Aug 6
Lima	Jul 6	Feb and Aug 21
Nandi	Aug 24	Feb and Aug 21
Townsville	Jul 18	Feb and Aug 15
Vacoas	Jul 27	Feb and Aug 6

The strongest easterlies, given by $du/dt=0$, occur generally in the last week of July over these areas.

Over the North Pacific Ocean and in the Southern Hemisphere solutions of $d^2u/dt^2=0$ are significantly later than over southern Asia and North Africa.

(iii) All the Southern Hemisphere stations display a solution of $d^2u/dt^2=0$ between December 9 and 30, corresponding to the commencement of summer circulations. Many Northern Hemisphere stations show a secondary solution of $d^2u/dt^2=0$ at about the same time, but at the other stations, mostly in southern Asia, d^2u/dt^2 exhibits only a minimum in winter and does not reach zero.

(iv) The other singularity in Southern Hemisphere upper flow-patterns is indicated by solutions of $d^2u/dt^2=0$ between mid-March and mid-April, corresponding to the weakening of summer circulations. Only over the western North Pacific Ocean do solutions of $d^2u/dt^2=0$ coincide approximately with those in the Southern Hemisphere, solutions at other Northern Hemisphere stations seeming to possess no clear relationship to flow-patterns elsewhere.

6. Phases of annual and semi-annual harmonics

The dates upon which $\sin [(2\pi/12)(t+\phi)]=+1$ are shown in Table 3, together with the dates upon which $\sin [(4\pi/12)(t+\phi)]=-1$.

At most Northern Hemisphere stations the dates corresponding to $\sin [(2\pi/12)(t+\phi)]=+1$ occur in late January or early February, which is consistent with the accepted view that at this time of year the tropospheric temperature contrast between low and high northern latitudes is most marked, and hence upper tropospheric westerly momentum should then be greatest (or easterly momentum least). Similarly, at most Southern Hemisphere stations the dates occur near mid-winter, but it will be noticed that the difference in the values of t for which $\sin [(2\pi/12)(t+\phi)]=1$ between Northern and Southern Hemispheres is not six months.

Over the western Pacific Ocean the above explanation does not appear to apply, for dates do not conform to the general tendency for $\sin [(2\pi/12)(t+\phi)]=+1$ to occur in mid-winter; this inconsistency deserves investigation.

The semi-annual harmonic exhibits only small differences of phase between localities, and periods during which $\sin [(4\pi/12)(t+\phi)]$ is negative coincide well with periods of monsoon activity over

TABLE 4

Values of A and $4B$ in m/sec, dates when $du/dt=0$ and the values of du/dt in m/sec / month when

(i) and $\sin \frac{2\pi}{12} (t+\phi) = +1$ ii) $\sin \frac{4\pi}{12} (t+\psi) = -1$

Station	A	$4B$	$du/dt=0$	(i)	du/dt (ii)
<i>North Africa & Arabia</i>					
Aden	18.1	23.8	Dec 15 Jan 27 Mar 6	-0.02	-0.02
Bahrein	24.1	20.5	Feb 9	+0.40	+0.51
Dakar	12.2	18.0	Dec 12 Feb 21 Mar 12	-1.23	-0.75
Fort Lamy	10.4	13.2	Mar 12	+0.69	+0.54
Khartoum	18.0	21.8	Mar 6	+1.08	+0.88
Port Sudan	22.8	23.8	Jan 6	-0.25	-0.25
<i>Asia</i>					
Calcutta	23.0	15.3	Jan 21	-0.42	-0.60
Hong Kong	21.8	9.6	Jan 30	+0.06	+0.40
Trivandrum	10.8	8.0	Feb 9	+0.41	+0.57
<i>Central America</i>					
Curacao	4.1	13.9	Nov 24 Feb 3 Apr 21	+1.25	+0.49
Juliana	7.3	15.6	Dec 9 Jan 30 Apr 12	+1.40	+0.75
Miami	16.6	8.8	Feb 15	+0.58	+1.23
Swan Island	9.3	6.7	Feb 9	0.00	0.00

southern Asia, North Africa and northern Australia.

Inspection of Table 3 shows that at several stations the dates upon which $\sin [(2\pi/12)(t+\phi)] = +1$ and $\sin [(4\pi/12)(t+\psi)] = -1$ occur within a few days of each other. For a coincidence Eq. (3) reduces to :

$$\frac{d^2u}{dt^2} = -\left(\frac{2\pi}{12}\right)^2 [A - 4B] \quad (4)$$

$$\text{and } \frac{du}{dt} = \frac{2\pi}{12} \left[A \cos \frac{2\pi}{12} (t + \phi) + 2B \cos \frac{4\pi}{12} (t + \psi) \right] = 0$$

There is, therefore, a turning point of the function $u=f(t)$, and for $u = \text{maximum}$, $d^2u/dt^2 < 0$ and $A > 4B$.

Stations for which Eq. (4) is a good approximation are listed in Table 4, together with (i) values of A and $4B$, (ii) dates during winter when $du/dt = 0$, and (iii) the values of du/dt corresponding to the dates upon which $\sin [(2\pi/12)(t+\phi)] = +1$ and $\sin [(4\pi/12)(t+\psi)] = -1$. It can be seen that for all stations yielding only two solutions of $d^2u/dt^2 = 0$ during the year (see Table 2) the condition $A > 4B$ is satisfied, whereas for all stations yielding four solutions $A < 4B$.

Where $A > 4B$ there is one maximum value of the function $u=f(t)$ and the winter part of the graph of $u=f(t)$ resembles Fig. 5(a), where, $A < 4B$, however, the graph of $u=f(t)$ resembles either

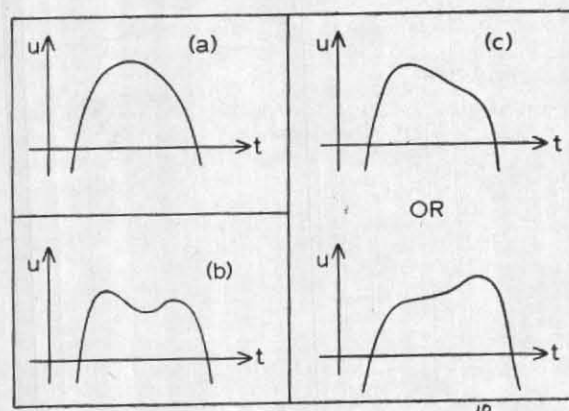


Fig. 5. The function $u=f(t)$, i.e., Eq. (2), plotted for winter months

Fig. 5(b) or Fig. 5(c). At the stations where Fig. 5(c) is appropriate a [maximum, positive, value of the function $d^2u/dt^2=f(t)$ accompanies the near coincidence of dates upon which $\sin [(2\pi/12)(t+\phi)] = +1$ and $\sin [(4\pi/12)(t+\psi)] = -1$ but, as Table 4 shows, du/dt is not simultaneously zero. It should be noted that values of ϕ and ψ were calculated to the nearest ± 0.1 month; although both dates given in Table 3 for Port Sudan are 30 January there is, in fact, a difference of about one day between them. This explains why the value of du/dt given for this station in Table 4 is not zero. For stations at which $A < 4B$, dates during winter when d^2u/dt^2 is maximum are listed in Table 5, together with the associated value of d^2u/dt^2 .

TABLE 5

For stations at which $A < 4B$, the date during winter when du^2/dt^2 is maximum and the associated value of du^2/dt^2

Station	Date of max.	Value
Aden	Jan 27	+1.57
Dakar	Feb 6	+1.60
Fort Lamy	Jan 27	+0.79
Khartoum	Jan 21	+1.05
Port Sudan	Jan 30	+0.26
Curacao	Feb 3	+2.69
Juliana	Feb 3	+2.32

Evidently the influence of the semi-annual harmonic can be sufficient to so counteract the

annual harmonic that westerly momentum is in fact greatest (or easterly momentum least) not in mid-winter but in early or late winter.

7. Concluding remarks

The purpose of this paper has been to report the results of the analyses, rather than to discuss their dynamical implications. It is clear that upper easterlies associated with summer monsoon circulations influence 100-mb wind patterns well beyond those areas generally considered by geographers to be monsoonal, on the basis of rainfall activity and surface-wind reversals.

Acknowledgement

I am very grateful to my wife for a great deal of computational assistance.

REFERENCES

- | | | |
|-------------------------------|------|--|
| Hantel, M. | 1971 | <i>J. Appl. Met.</i> , 10 , 5, pp. 875-881. |
| Struning, J. O. and Flohn, H. | 1969 | <i>Bonn. Met. Abh.</i> , Heft 10. |
| Van Loon, H. and Jenne, R. L. | 1969 | <i>J. Atmos. Sci.</i> , 26 , pp. 218-232. |
| | 1970 | <i>Tellus</i> , 22 pp. 391-398. |

APPENDIX

Key to stations whose location is shown in Fig. 2 and, in brackets, the number of observations analysed (months)

Ab	Abidjan	05°15' N	03°56' W	(84)	Ko	Koror	07° 20' N	134° 29' E	(132)
Ad	Aden	12 50 N	45 01 E	(84)	L	Lima	12 01 S	77 07 W	(48)
B	Bahrein	25 16 N	50 37 E	(132)	M	Miami	25 48 N	80 16 W	(132)
Ba	Bangkok	13 44 N	100 30 E	(72)	Ma	Malta	35 50 N	14 27 E	(132)
Bu	Bulawayo	20 09 S	28 37 E	(108)	Mi	Minamidaitcuma	25 50 N	131 14 E	(72)
BH	Broken Hill	14 27 S	28 28 E	(96)	Mj	Majuro	07 05 N	171 23 E	(108)
C	Curacao	12 11 N	68 59 W	(132)	Mk	Malakal	09 33 N	31 39 E	(84)
Ca	Calcutta	22 39 N	88 27 E	(72)	MI	Mareus Island	24 18 N	153 58 E	(60)
Ch	Chiengmai	18 47 N	98 59 E	(36)	N	Nandi	17 45 S	177 27 E	(60)
Cn	Canton Island	02 46 S	171 43 W	(84)	ND	New Delhi	28 35 N	77 12 E	(60)
Cy	Cloncurry	20 40 S	140 30 E	(72)	P	Ponape	06 58 N	158 13 E	(120)
CI	Cocos Island	12 05 S	96 53 E	(72)	PS	Port Sudan	19 35 N	37 13 E	(84)
D	Dakar	14 44 N	17 30 W	(84)	S	Singapore	01 21 N	103 54 E	(120)
Da	Darwin	12 26 S	130 52 E	(72)	Sa	Saigon	10 49 N	106 40 E	(84)
E	Ocean Weather Ship 'E'	35 00 N	48 00 W	(108)	So	Songkhla	07 11 N	100 37 E	(72)
FL	Fort Lamy	12 08 N	15 02 E	(72)	SI	Swan Island	17 24 N	83 56 W	(132)
G	Gibraltar	36 09 N	05 21 W	(132)	Tk	Truk	07 28 N	151 51 E	(132)
Gu	Guam	13 33 N	144 50 E	(132)	To	Tobruk	32 05 N	23 59 E	(120)
HK	Hong Kong	22 19 N	114 10 E	(96)	Tr	Trivandrum	08 29 N	76 57 E	(48)
J	Juliana	18 02 N	63 06 W	(132)	Tw	Townsville	19 15 S	146 46 E	(72)
K	Kwajalein	08 43 N	167 44 E	(72)	U	Ubon Ratchathani	15 15 N	104 53 E	(48)
	Khartoum	15 36 N	32 33 E	(84)	V	Vacoas	20 18 S	57 30 E	(36)
					Y	Yap	09 31 N	138 08 E	(96)